Title

Toxic Tides and Environmental Injustice: Social Vulnerability to Sea Level Rise and Flooding of Hazardous Sites in Coastal California

Journal

Environmental Science and Technology, 57(19)

ISSN

0013-936X

Authors

Cushing, Lara J
Ju, Yang
Kulp, Scott
et al.

Publication Date

2023-05-16

DOI

10.1021/acs.est.2c07481

Peer reviewed

Environmental Science & Technology

pubs.acs.org/est

Article

Toxic Tides and Environmental Injustice: Social Vulnerability to Sea Level Rise and Flooding of Hazardous Sites in Coastal California

Lara J. Cushing,* Yang Ju, Scott Kulp, Nicholas Depsky, Seigi Karasaki, Jessie Jaeger, Amee Raval, Benjamin Strauss, and Rachel Morello-Frosch*

Cite This: *Environ. Sci. Technol.* 2023, 57, 7370−7381

Read Online

ACCESS | Metrics & More | Article Recommendations | Supporting Information

ABSTRACT: Sea level rise (SLR) and heavy precipitation events are increasing the frequency and extent of coastal flooding, which can trigger releases of toxic chemicals from hazardous sites, many of which are in low-income communities of color. We used regression models to estimate the association between facility flood risk and social vulnerability indicators in low-lying block groups in California. We applied dasymetric mapping techniques to refine facility boundaries and population estimates and probabilistic SLR projections to estimate facilities' future flood risk. We estimate that 423 facilities are at risk of flooding in 2100 under a high emissions scenario (RCP 8.5). One unit standard deviation increases in nonvoters, poverty rate, renters, residents of color, and linguistically isolated households were associated with a 1.5−2.2 times higher odds of the presence of an at-risk site within 1 km (ORs [95% CIs]: 2.2 [1.8, 2.8], 1.9 [1.5, 2.3], 1.7 [1.4, 1.9], 1.5 [1.2, 1.9], and 1.5 [1.2, 1.9], respectively). Among block groups near at least one at-risk site, the number of sites increased with poverty, proportion of renters and residents of color, and lower voter turnout. These results underscore the need for further research and disaster planning that addresses the differential hazards and health risks of SLR.

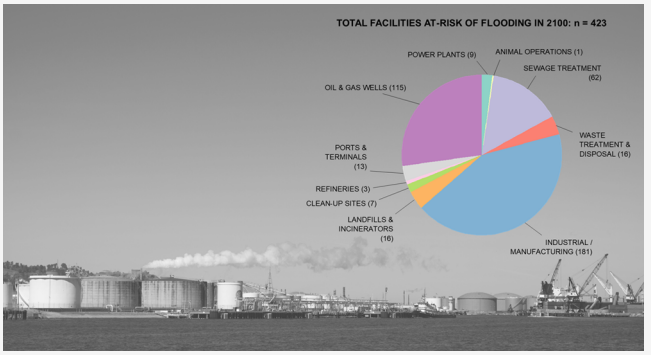

KEYWORDS: *GIS, climate change, environmental equity, exposure analysis, participatory research, climate resilience*

INTRODUCTION

The frequency of extreme coastal flooding across much of the world is projected to more than double by 2050 due to sea level rise (SLR).[1] In California, SLR has closely mirrored global average rates of about 0.3 cm per year over the past several decades.[2] Assuming greenhouse gas emissions continue to rise, SLR of 0.2 to 0.5 m is expected between 2000 and 2050 and 0.5 to 1.4 m by the end of the century.[3] These projections pose significant implications for coastal communities in California where more than 68,000 people live within 0.3 m elevation of the local mean high tide line, and more than 145,000 live within 0.9 m.[4] In the coming decades, even larger areas will experience coastal flooding during high tides, storm surges, high precipitation, and El Niño events due to higher average sea levels.[5]

Past flood and storm surge events have led to releases of toxic substances into the environment from industrial, hazardous waste, and legacy contamination sites.[6−8] For example, flooding caused by Hurricanes Katrina and Rita resulted in an estimated 166 releases of hazardous substances, largely due to emergency shut down and start-up operations at industrial facilities.[9−11] SLR-amplified flood heights of future storm surges and tidal events will increase flood risks at hazardous sites in coastal areas and the possibility of similar natural hazard-triggered technological ("natech") disasters.[12,13] Less severe flooding can also contribute to contaminant releases via damage from debris flow, corrosion of pipelines and other infrastructure, power failures, and impediments to operator access.[14]

Flood-induced contaminant releases are more likely to impact low-income households and people of color because they are more likely to live near industrial and hazardous waste facilities.[15−18] Socially disadvantaged communities also have fewer resources to anticipate, mitigate, cope with, or recover from the effects of flooding. Prior research shows people of color and the poor are less likely than others to own a car enabling evacuation, more likely to suffer injury or die during the aftermath of an extreme flood event, and less likely to return and rebuild afterward.[19−21] In the case of Hurricane Harvey, pollutant releases from petrochemical facilities associated with flooding disproportionately impacted neigh-

Received: October 11, 2022
Revised: March 17, 2023
Accepted: March 20, 2023
Published: May 2, 2023

borhoods with higher proportions of low income and Hispanic residents.[8]

In this analysis, we present the first assessment, of which we are aware, of the number and location of hazardous facilities at risk of future flooding due to SLR in California and assess the environmental justice implications. We consider a wide variety of sites that have hazardous substances on site and have documented excess contaminant releases to air, land, and floodwaters during previous flood events, including refineries, industrial facilities, and sewage treatment plants, as well as cleanup sites where SLR may cause changes in groundwater movement that leads to the spread of below-ground hazardous substances. We combine information on the location of hazardous sites and present-day population demographics with SLR projections to assess inequalities in future flood risk projections under two greenhouse gas emissions scenarios. We consider proximity to sites at-risk of flooding in 2050 and 2100 with respect to current community demographics and indicators of social vulnerability to characterize inequities in potential exposure and test the hypotheses that (1) SLR will increase the number of sites at risk of a 1-in-100 year flood in 2050 and 2100 and (2) vulnerable and socially marginalized populations are more likely to live near at-risk sites.

We collaborated with an advisory committee comprised of environmental justice advocates working on community-based climate resilience strategies in the San Francisco Bay Area, Central Coast, and Southern California who provided guidance on the study design, methods, interpretation, and dissemination of results. This community-engaged strategy sought to facilitate translation of our analytical results to inform policy and resilience planning in vulnerable regions throughout California. Such integration of data- and community-driven methods also allows for ground-truthing of analytical results, thus enhancing methodological rigor, public relevance, and policy reach of the research more broadly.[22−24]

MATERIALS AND METHODS

Project methods were codeveloped in partnership with a five-member advisory committee, starting with the development of a funding proposal to support the work and continuing in an iterative process through the study design, implementation, and development of online data visualization tools for results dissemination. Committee members were staff of organizations focused on environmental justice, public health, and climate change and working on climate resilience policy. Following an initial in-person meeting, we interacted with the committee virtually, due to the COVID-19 pandemic, through a series of regular and ad-hoc meetings to gain feedback on our study design and research methods including data cleaning, metrics development, statistical analysis, and interpretation of results. We collectively chose the greenhouse gas emissions scenarios, timeframes (2050 and 2100), and range of SLR estimates we would investigate, as well as the flood risk metrics, categorization of sites considering both their potential hazards and ease of interpretation, and the demographic and social vulnerability metrics to include. One advisory board member (A. Raval) contributed to the writing of this manuscript. The committee also coordinated and hosted a series of four public webinars (one state-wide, one each in the San Francisco Bay Area, Central Coast, and Southern California regions) to share preliminary findings and gather feedback from a broader range of roughly 350 community and agency stakeholders. Feedback received via these webinars resulted in the addition of more extreme SLR scenarios in our study to align with statewide guidance and considerations of groundwater movement.

Hazardous Sites. We compiled data on the location of active industrial facilities and other potentially hazardous sites from four sources: the U.S. Environmental Protection Agency's (EPA) Facility Registry Service (FRS),[25] the U.S. Energy Information Administration's (EIA) Energy Atlas,[26] the U.S. Army Corp of Engineers' (USACE) Waterborne Commerce Statistics Center,[27] and the Enverus database[28] of active oil and gas well permits (Table 1). To ensure we captured all sites from these sources with potential SLR-related flood risk, we included sites located in any of the 29 California counties containing land area within a 3 km Euclidean distance of the 10 m elevation above the current high tide line (see Supporting Information, Figure S1 study area map). The FRS compiles information from more than 30 national and 45 state data systems on facilities subject to federal environmental regulation in the United States. We excluded FRS records with poor locational information. This included records with horizontal accuracy values greater than 50 m or imprecise location descriptions (e.g., latitude and longitude coordinates derived from zip codes). To focus the analysis on sites most likely to pose risks of SLR-related contaminant releases, we also excluded records with a "site type name" indicating that contamination had been remediated ("contamination addressed") or where the "active status" was classified as "No", "Closed", "Permanently Closed", "Retired", or "Permanently shut down, Cancelled, Postponed, or No Longer Planned", or sites with "environmental interest" end dates before 2020, indicating the site was no longer regulated under a given environmental interest type. We chose to retain inactive facilities and facilities with expired permits ("active status" is "inactive" or "expired") because residual hazardous materials may remain at these sites.

We then classified FRS sites into one of 7 mutually exclusive categories using (1) the environmental permits or regulatory programs ("environmental interest") given in the FRS; (2) the North American Industry Classification System (NAICS) code; and/or (3) keyword filters (see Supporting Information Table S1 for details). We applied a hierarchy to ensure that each category was mutually exclusive and to eliminate duplicate entries, because many FRS sites have multiple environmental permits and/or NAICS codes and thus multiple records in the FRS.

FRS data were supplemented with information on petroleum refineries from the EIA Energy Atlas. To ensure petroleum refineries were not duplicated between the FRS and EIA data sets, we manually identified and removed all refineries contained in the EIA data set from the FRS data set using facility names and coordinates. Additional fossil fuel infrastructure was included from the EIA Energy Atlas (petroleum product terminals and crude oil rail terminals) and USACE data set (petroleum ports). Finally, we obtained active oil and gas well locations from Enverus and filtered based on production type to limit to production or stimulation wells (see Supporting Information Table S2 for details).

Active oil and gas well locations were represented as points based on the longitude and latitude coordinates provided by Enverus. All other sites were regeocoded using the Google API and joined to tax parcel data from DMP LightBox to better approximate the geographic extent of each site from its geographic coordinates.[29] Roughly 80% of these newly geocoded site locations fell within tax parcel boundaries; we

https://doi.org/10.1021/acs.est.2c07481
Environ. Sci. Technol. 2023, 57, 7370−7381

Table 1. Sites and Data Sources Included in the Analysis (N = 10,390)[a]

category	source	count	description
power plants (nuclear and fossil fuel)	EPA Facility Registry Service (FRS)	79	electricity generating facilities that provide power to the electric grid using primarily nuclear, coal, oil, gas, or other fossil fuels
animal operations	FRS	42	facilities primarily engaged in feeding cattle for fattening, milking dairy cattle, or concentrated animal feeding operations (CAFOs)
sewage treatment facilities	FRS	341	operating sewer systems or sewage treatment facilities that collect, treat, and dispose of waste
hazardous waste treatment and disposal	FRS	107	facilities designated for the treatment and/or disposal of hazardous waste or establishments primarily involved in the combined activity of collecting and/or hauling of hazardous wastes within a local area and operating treatment or disposal facilities for hazardous waste
Toxic Release Inventory facilities	FRS	3595	facilities required to report to the Toxic Release Inventory (TRI) that handle, manufacture, use, or store certain flammable or toxic substances
solid waste landfills and incinerators	FRS	271	operating landfills, combustors, and/or incinerators designated for the disposal of nonhazardous solid waste
cleanup sites and sites with radioactive material	FRS	68	contaminated sites including military sites (BRAC), Superfund sites on the National Priorities List (NPL), and sites with radioactive contamination, radionuclide emissions, or involved in radioactive waste disposal are also included.
refineries	EIA U.S. Energy Atlas	13	facilities involved in the manufacture of fossil fuels
fossil fuel ports and terminals	EIA U.S. Energy Atlas & USACE Waterborne Commerce Statistics Center	66	facilities involved in the transport of fossil fuels
active oil and gas wells	Enverus	5808	active oil and gas wells used for production or enhanced oil recovery

[a]Categories are mutually exclusive, and sites that could fall into more than one category were assigned using the hierarchy of categories as listed in descending order.

assumed the intersecting parcel geometries approximated the extents of these sites and used the resulting polygons in our subsequent flood risk projections. The remaining 20% of sites did not intersect tax parcels, usually because their point locations were along roadways adjacent to the facility property. For these sites, we calculated the median parcel area by site category based on those sites that intersected parcels. We then created a circular buffer equal to the corresponding median areas by category to estimate site extents at these locations (see schematic Supporting Information Figure S2). Parcels and circular buffer areas that extended beyond the mean high tide line were clipped at the coast.

In a final round of data cleaning, we removed 139 duplicate sites that 1) were part of the same category and 2) had identical coordinates after geocoding and 3) the same or a similar address (based on a fuzzy text match). We retained those facilities with identical coordinates and similar addresses if they were assigned to different categories (n = 15). We dropped facilities with identical coordinates in the same category if they had different addresses (n = 14) because we determined geocodes were inaccurate upon visual inspection for these sites.

The final facilities data set consisted of 10,390 sites in 29 California counties, classified into the following categories: nuclear and fossil fuel power plants (n = 79), animal operations (n = 42), sewage treatment facilities (n = 341), hazardous waste treatment and disposal (n = 107), Toxic Release Inventory (TRI) facilities (n = 3,595), landfills and incinerators (n = 271), cleanup sites (including National Priority List Superfund sites and sites with radioactive material; n = 68), refineries (n = 13), fossil fuel ports and terminals (n = 66), and oil and gas wells (n = 5808) (Table 1).

Sea Level Rise and Flood Risk Projections. To assess site vulnerability, we followed the method described by Kulp and Strauss[30] and Buchanan et al.[31] In brief, our analyses used probabilistic sea level rise projections[32] assuming low (Reference Concentration Pathway [RCP] 4.5) and high (RCP 8.5) greenhouse gas emission scenarios for the years 2050 and 2100. These projections incorporated local vertical land movement, such as subsidence caused by tectonic activity, large-scale underground fluid extraction, and glacial isostatic adjustment. Coastal flood height return level curves from Tebaldi et al.[33] are defined at each of seven U.S. tide stations in California with more than 30 years of hourly water level records.

In these analyses, we estimate $P_{annual}(H \geq Elev_i \mid Y = y)$, the total annual probability P of *at least one* coastal flood exceeding the land elevation $Elev_i$ of each site € in year y, integrated across the full distribution of SLR projections for each emissions scenario. In this context, we defined $Elev_i$ as the 25th percentile of land elevation within the parcel/circular buffer of site i. We derived land elevations from NOAA's Coastal Topographic Lidar digital elevation model[34] and refined the Buchanan et al. approach[31] to better incorporate levees and other flood control structures. Hydrological connectivity to the ocean was enforced.

We applied eq (1) from Buchanan et al.,[30,31] which integrates the localized SLR projections and flood risk statistics, to estimate these annual probabilities. We considered sites to be at-risk if their projected annual probabilities exceeded 0.01 (i.e., threatened by a 1-in-100 year flood event). Furthermore, by summing these probabilities across administrative areas (e.g., across block groups), we derived that area's

https://doi.org/10.1021/acs.est.2c07481
Environ. Sci. Technol. 2023, 57, 7370−7381

total expected annual exposure (EAE) or the expected number of hazardous sites exposed in a given year.

Extreme SLR Scenarios and Groundwater Encroachment. Our main analysis using RCP 8.5 corresponds to a central projection of about 0.9 m of SLR by 2100. To facilitate integration of our findings into state-level climate resilience planning, we additionally estimated how many facilities would be at risk of inundation under more extreme levels of SLR in accordance with California agency guidance documents recommending consideration of 6.9 feet (~2.1 m) of SLR ("Medium Risk-Aversion" scenario for residential and commercial development) and 10.1 feet (~3.1 m) of SLR ("High-Risk Aversion" scenario for critical infrastructure).[35,36] For our analysis of "extreme" scenarios, site risk was classified on a yes/no basis depending on each site's elevation and connectivity to the sea.

Rising groundwater due to SLR may lead to groundwater emergence and the movement of contaminated groundwater inland.[37] This movement can affect the release and spread of surface and subsurface toxic substances at contaminated sites.[38] We integrated data on projected groundwater depths available in half meter increments of SLR from the U.S. Geological Survey.[39] We used groundwater rise estimates corresponding most closely to the degree of SLR in the two extreme scenarios above: 2 m (~6.6 feet) and 3 m (~9.8 feet). We followed published guidance to select the parameters of the groundwater modeling data (i.e., the Mean Higher-High Water marine boundary condition and a horizontal hydraulic conductivity of 1.0 m/day).[40] We considered a site to be at-risk of groundwater encroachment if it spatially overlapped with groundwater tables 1 m or less below the surface.

Community Demographics and Social Vulnerability Measures. We estimated the following census block-group level measures using the U.S. Census American Community Survey's (ACS) 2013−2017 five-year estimates:[41] age (% under the age of 18 and % 65 and older), race/ethnicity (% people of color, defined as the inverse of % non-Hispanic White), poverty (% below twice the federal poverty line), housing tenure (% renters), vehicle ownership (% of households without a vehicle), family structure (% single parent-headed households), linguistic isolation (% of households where no one 14 years or older speaks English "very well"). We derived a presence/absence measure of affordable housing (market-based or government subsidized) using data from CoStar and Urban Land Institute's 2017 Naturally Occurring Affordable Housing Analysis and the National Housing Trust's 2017 Affordable Housing Programs.[31,42] We used voter turnout data from California's Statewide Database[43] on redistricting to derive the percent of registered voters who voted during the 2016 general elections as an indicator of civic engagement, following Maizlish's (2016) methodology.[44] Finally, we used CalEnviroScreen 4.0 to identify disadvantaged communities.[45] CalEnviroScreen is a relative ranking of California census tracts that combines indicators of pollution burden from multiple environmental hazards and population vulnerability to pollutant exposures. We defined disadvantaged communities as census tracts with the highest quartile of cumulative environmental burdens and social vulnerability (in keeping with an earlier version of CalEnviroScreen) but with updated CalEnviroScreen 4.0 cumulative impact percentiles.[46]

We then took this population data and geographically refined it to a higher spatial resolution using dasymetric mapping methods to define exposed blocks groups and characterize populations near at-risk sites (see Supporting Information Figure S2, schematic illustration of definition of exposed block groups). Dasymetric mapping refers to the disaggregation of spatial data—in this case census block boundaries—to finer spatial units of analysis using ancillary data. It has been used in prior environmental justice and sea level rise vulnerability analyses[47,48] and helps to accurately distinguish between residences and unpopulated space, especially in sparsely populated settings where census blocks (the smallest census geographic unit) can still be relatively large (>50 km^2). This approach helps to ensure our analysis focuses on the places where people live and reduces measurement error in the estimation of distance between residences and hazardous sites at risk. Our method was utilized and is detailed further elsewhere.[17,49,50] Briefly, we created a high-resolution (i.e., sub-block) map of populations residing near potentially hazardous facilities of resolution that was comparable to the facility boundaries and digital elevation data we used; this entailed developing a statewide, 100 m-resolution "target" population grid within census blocks for which population counts were observed in the 2010 census, using two ancillary data sources: (1) a statewide database of more than 12 million individual tax parcel boundaries from DMP LightBox[29] and (2) spatial building footprint data for nearly 11 million buildings in California. The latter is part of a nationwide layer developed by Microsoft using satellite imagery and machine learning classification techniques.[51]

Within each census block, population was apportioned to small residential parcels and/or building footprints following a tiered approach. First, we identified all residential parcels within each census block based on land use descriptions provided in the statewide parcel data set. If residential parcels were identified in a given block and relatively small (<1 acre or roughly 4047 m^2), we assumed its population to be located within these residential areas alone. This parcel-based apportionment accounted for 91.8% of California's population. Second, for blocks containing no small residential parcels but with a nonzero population count according to the 2010 Census, we allocated population evenly across all building footprint areas identified within them. This was common for blocks in wilderness areas or zones of low-density agriculture, with parcels classified as "open space" or "agricultural" in the statewide parcel database, but which still contain residences. This building footprint-based apportionment accounted for 7.9% of California's population.

Finally, for the remaining census blocks that contained neither residential parcels nor building footprints but had a nonzero population count, we assumed that population counts were evenly distributed across the entire block area. This "default" method of population apportionment was applied to 0.3% of the state's population. Population values apportioned to these target zones within each block were based on 2010 decennial census values at the block-level but scaled to match the 2013−2017 ACS vintage based on population growth rates observed in parent block-groups between the 2010 census and the 2013−2017 ACS.

Analytic Approach. We first examined the distribution of at-risk sites by county, year, and emissions scenario for the 10,390 facilities in 29 counties. Further analysis focused on the 18 counties from our initial universe with at least one site at risk under RCP 8.5 by 2100. We conducted a block-group-level analysis that included all block groups within a 3-km Euclidean distance of the 10-m elevation line in these 18 counties

https://doi.org/10.1021/acs.est.2c07481
Environ. Sci. Technol. 2023, 57, 7370−7381

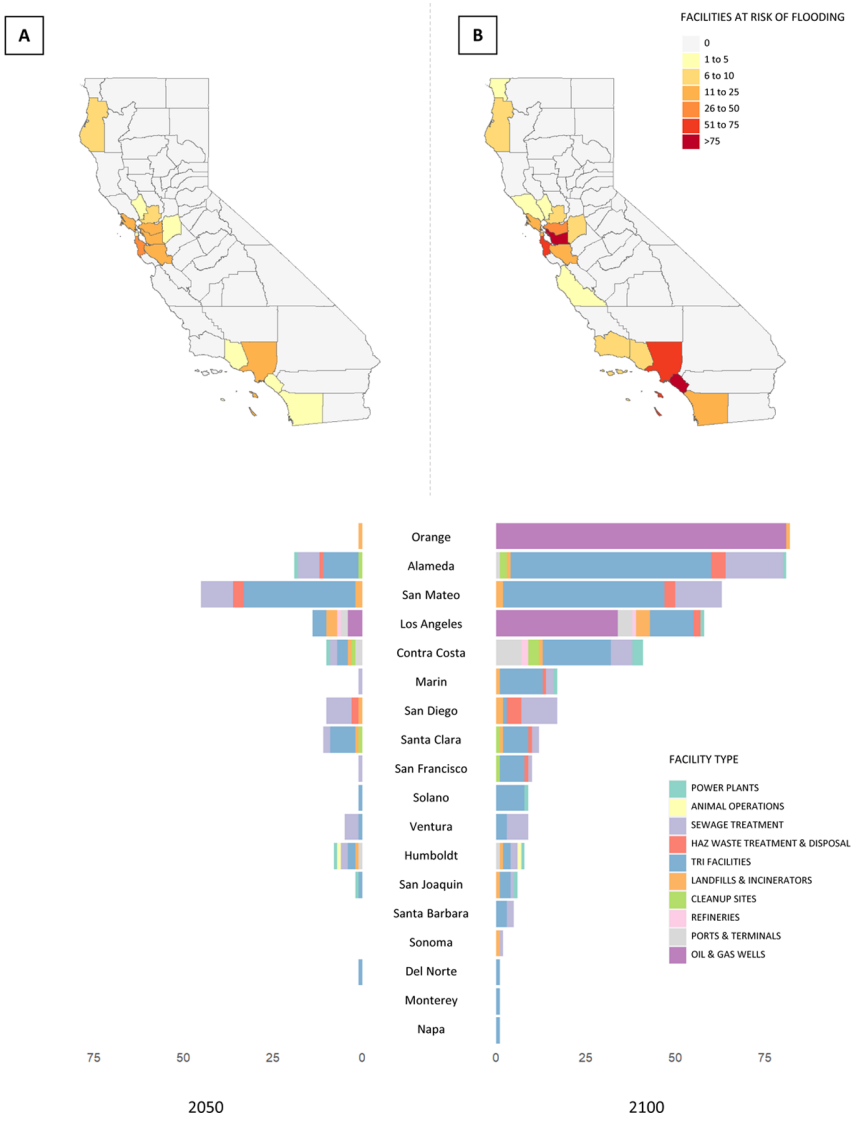

Figure 1. Number of sites at risk of flooding due to SLR in (a) 2050 and (b) 2100 under a high emissions scenario (RCP 8.5) by county and type.

(hereafter "low-lying" block groups). For the main analysis, exposed block groups were defined as those low-lying block groups with dasymetrically mapped populated areas within one kilometer of at least one at-risk site (see Supporting Information Figure S2 schematic). In sensitivity analyses, we used a 3-km buffer to define exposed block groups. We examined two additional outcome variables for each exposed block group: the total number of at-risk sites and sum of annual flood event probabilities (the area's expected annual exposure, EAE) from all at-risk sites nearby. Following a similar logic to our definition of exposed block groups, we only kept sites (n = 5,914 and 5,921 respectively) that were within 1 or 3 km from populated areas when calculating outcome variables for each block group.

We derived descriptive statistics and correlation coefficients between each social vulnerability indicator and our outcomes. We then conducted a series of multivariate regression models that included one vulnerability indicator, block-group population density (people per square kilometer), and county fixed effects as independent variables. We included population density as a potential confounder given prior research demonstrating an association between population density and the likelihood of a proximate industrial facility, and since disadvantaged populations tend to be more densely populated.[52,53] We included county fixed effects to control for regional demographic differences and to compare block groups with and without at-risk sites within the same coastal county. We scaled vulnerability indicators by unit standard deviation (SD) using the mean and SD from block groups in the 18 counties to facilitate comparisons across indicators. We did not include multiple vulnerability indicators in the same model due to multicollinearity (see Supporting Information Figure S3 correlation coefficients). We used a logistic model to estimate the odds of an at-risk site nearby (yes/no variable), a negative binomial model to estimate the number of sites nearby (count variable), and a linear model to estimate EAE (continuous variable). Models of the number of at-risk sites and EAE only included the subset of block groups that had at least one at-risk site within one kilometer (exposed block groups). We estimated county clustered robust standard errors to control for the spatial autocorrelation.

Finally, we used generalized additive models to examine nonlinear associations between the continuous vulnerability indicators and our outcomes. For the logistic model estimating

https://doi.org/10.1021/acs.est.2c07481
Environ. Sci. Technol. 2023, 57, 7370−7381

Table 2. Number and Type of Sites at Risk of SLR-Related Flooding by Scenario and Year Across 29 California Counties

		no. (%) at risk, RCP 4.5		no. (%) at risk, RCP 8.5	
category	no. of facilities in analysis	2050	2100	2050	2100
power plants (nuclear and fossil fuel)	79	3 (3.8)	9 (11.4)	4 (5.1)	9 (11.4)
animal operations	42	1 (2.4)	1 (2.4)	1 (2.4)	1 (2.4)
sewage treatment facilities	341	33 (9.7)	57 (16.7)	34 (10.0)	62 (18.2)
hazardous waste treatment and disposal	107	6 (5.6)	14 (13.1)	6 (5.6)	16 (15.0)
Toxic Release Inventory facilities	3595	59 (1.6)	145 (4.0)	61 (1.7)	181 (5.0)
solid waste landfills and incinerators	271	10 (3.7)	15 (5.5)	10 (3.7)	16 (5.9)
cleanup sites and sites with radioactive material	68	3 (4.4)	6 (8.8)	3 (4.4)	7 (10.3)
refineries	13	1 (7.7)	2 (15.4)	1 (7.7)	3 (23.1)
fossil fuel ports and terminals	66	5 (7.6)	10 (15.2)	5 (7.6)	13 (19.7)
active oil and gas wells	5808	4 (0.1)	113 (1.9)	4 (0.1)	115 (2.0)
total	10390	125 (1.2)	372 (3.6)	129 (1.2)	423 (4.1)

Table 3. Distribution of Community Characteristics within Low-Lying Block Groups with and without at-Risk Sites within 1 km in 2100 under RCP 8.5 across 18 California Counties (n = 7,211)

	no. of at-risk sites (n = 6,381)[a] total population: 10,154,202 median [25th, 75th percentile]	≥1 at-risk site (n = 831)[a] total population: 1,388,531 median [25th, 75th percentile]	P-value[b]
% voters not voting	23.9 [17.6, 30.9]	27.0 [18.9, 35.8]	<0.01
% poverty	22.1 [12.0, 38.7]	29.4 [15.5, 51.2]	<0.01
% of renter-occupied units	43.5 [22.9, 68.7]	52.9 [30.6, 75.6]	<0.01
% people of color	57.1 [33.2, 81.0]	68.9 [42.4, 86.7]	<0.01
% linguistic isolation	5.2 [1.0, 12.2]	7.3 [2.7, 15.3]	<0.01
% without a car	4.1 [1.2, 10.1]	6.3 [1.9, 13.9]	<0.01
% single parent household	15.3 [8.8, 24.7]	17.2 [9.5, 28.7]	<0.01
% elderly	21.2 [11.4, 35.5]	23.6 [13.0, 38.8]	<0.01
% under 18	20.0 [14.6, 25.5]	21.1 [14.0, 27.4]	0.01

[a]N is slightly lower for some individual vulnerability indicators due to missing data. [b]The P-value is from the Mann−Whitney U-test.

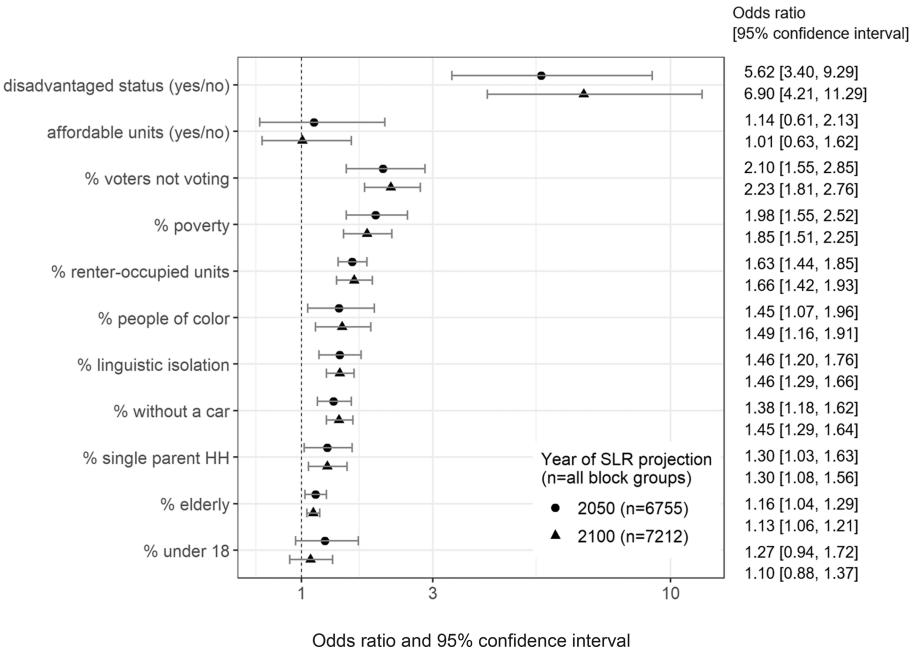

Figure 2. Association between individual block group vulnerability factors and the presence-absence of an at-risk site within 1 km among all low-lying block groups. Models considered one vulnerability factor at a time. All models controlled for population density and county fixed effects. Disadvantaged status (as defined by CalEnviroscreen) and presence of affordable housing are binary predictors; all other variables are continuous and were scaled by unit standard deviation to facilitate comparisons. Confidence intervals were calculated using robust standard errors. The dashed line indicates no association.

https://doi.org/10.1021/acs.est.2c07481
Environ. Sci. Technol. 2023, 57, 7370−7381

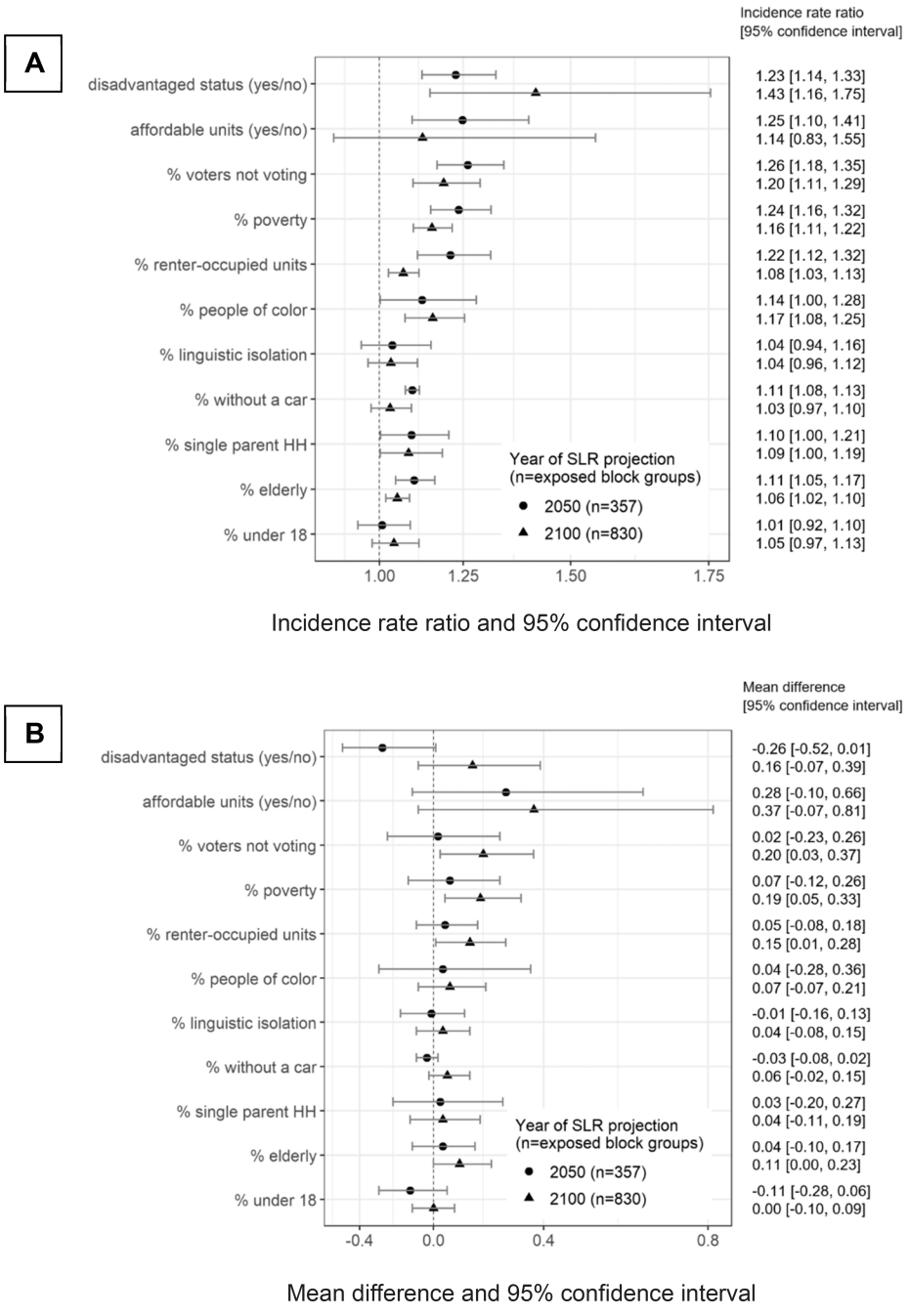

Figure 3. Association between individual block group vulnerability factors and (a) the total number of at-risk sites within 1 km and (b) the sum of EAE across sites within 1 km, among exposed block groups. Models considered one vulnerability factor at a time. All models controlled for population density and county fixed effects. Disadvantaged status (as defined by CalEnviroscreen 4.0) and presence of affordable housing are binary predictors; all other variables are continuous and were scaled by unit standard deviation to facilitate comparisons. Confidence intervals were calculated using robust standard errors. The dashed line indicates no association.

the odds of an at-risk site nearby and the binomial model estimating the number of at-risk sites nearby, we assessed whether the associations were nonloglinear. For the linear model estimating EAE across at-risk sites, we assessed whether the association was nonlinear. In the generalized additive models, we applied a penalized splines function to create smooth terms for the vulnerability indicators, through which nonlinearity was tested. Similar to earlier models, we also included county fixed effects and population density. We used effective degrees of freedom (edf) and its significance for the smooth terms to assess the significance of nonlinearity. An edf value closer to one indicates linearity, whereas higher values indicate nonlinearity.

RESULTS

Of the 29 counties considered in our analysis, 14 and 18 contained at-risk sites in 2050 and 2100, respectively, under the high emissions (RCP 8.5) scenario, with the San Francisco Bay Area and Los Angeles/Orange County regions having the highest total number of at-risk sites (Figure 1). Under the high emissions scenario, 129 (1.2%) sites were estimated to be at risk in 2050, and 423 (4.1%) sites were estimated to be at risk

https://doi.org/10.1021/acs.est.2c07481
Environ. Sci. Technol. 2023, 57, 7370−7381

in 2100 (Table 2). The largest number of at-risk sites were TRI facilities and oil and gas wells (Table 2). By 2100, roughly a fifth of coastal California sewage treatment facilities, refineries, and fossil fuel ports and terminals were estimated to be at-risk under the scenario of continued high greenhouse gas emissions. Under the low emissions scenario (RCP 4.5), 51 fewer sites were found to be at risk in 2100 (a 12% reduction; Table 2).

Under more extreme levels of sea level rise in accordance with California guidance for a medium- risk aversion, 603 (5.8%) facilities were projected to be at risk of coastal flooding, and we estimated that groundwater would encroach to <1 m below the surface of an additional 199 sites (Supporting Information Table S3). Under California's high-risk aversion scenario, we identified 736 (7.1%) facilities at risk of coastal flooding and an additional 173 with projected groundwater encroachment.

On average, populations living near (<1 km) at-risk sites had higher proportions of residents living in poverty, residents of color, renters, linguistically isolated households, elderly populations (defined as age 65 and older), children (defined as < 18 years old), single parent households, lower voter turnout, and lower car ownership (Table 3). In multivariate models considering the high emissions scenario (RCP 8.5), all vulnerability factors except % under age 18 and the presence of affordable housing were associated with an increased odds of an at-risk site within 1 km in both 2050 and 2100 (Figure 2). Disadvantaged community status as defined by CalEnviroScreen 4.0 was the most strongly associated with the presence of an at-risk site, with disadvantaged status being associated with a nearly 7-fold increase in the odds of an at-risk site within 1 km in 2100. This was followed by low voter turnout, poverty, housing tenure, race/ethnicity, linguistic isolation, vehicle ownership, single parent households, and elderly (see Supporting Information Table S4 for full model results).

When limiting our analysis to the universe of exposed block groups (with at least one at-risk site), the number of at-risk sites within 1 km was also unequally distributed with respect to all vulnerability factors except linguistic isolation and % under 18 (Figure 3a). Lower voter turnout and disadvantaged community status were the most strongly associated with the number of at-risk sites within 1 km (incidence rate ratio (IRR) and 95% CI: 1.3 [1.2, 1.4] in 2050 and 1.2 [1.1, 1.3] in 2100 per unit SD increase in % of voters not voting and 1.2 [1.1, 1.3] in 2050 and 1.4 [1.2, 1.8] in 2100 for disadvantaged vs not disadvantaged communities), followed by poverty, residents of color, and housing tenure (see Supporting Information Table S5 for full model results).

Flood risk severity as measured by EAE across all at-risk sites within 1 km was not as strongly associated with most of the vulnerability factors we considered when comparing among exposed block groups (Figure 3b). Lower voter turnout, poverty, and housing tenure were however all associated with increased mean EAE in 2100. A one unit SD increase in the % of residents living in poverty was associated with a 0.19 higher mean EAE (95% CI [0.05, 0.33]). An SD unit increase in the % of voters not voting and % of renters was associated with a 0.20 (95% CI [0.03, 0.37]) and 0.15 (95% CI [0.01, 0.28]) higher mean EAE, respectively (see Supporting Information Table S6 for full model results).

We found little evidence of non(log)linear associations (edf close to 1) between our vulnerability indicators and the outcomes with a few exceptions (Supporting Information, Figure S4). For example, we found that the association between % residents of color and odds of an at-risk site within 1 km was nonmonotonic in both 2050 (Supporting Information, Figure S4(a)) and 2100 (Supporting Information, Figure S4(b)), with the relationship being generally negative in block groups with less than 20% residents of color, but positive for the rest of the block groups. We found similar patterns between % population under age 18 and the odds of an at-risk site within 1 km. When looking at the sum of EAE across all at-risk sites within 1 km, we saw nonmonotonic associations between % voters not voting in 2050 (Supporting Information, Figure S4(e)) and between % elderly and sum of EAE across all at-risk sites in 2100 (Supporting Information, Figure S4(f)).

Findings from the sensitivity analysis considering a 3 km buffer distance to define exposed block groups were largely consistent in terms of the direction and statistical significance of associations with our vulnerability metrics (Supporting Information Tables S4−S6). Effect estimates were in general slightly attenuated in both 2050 and 2100 in the comparison of the odds of a nearby at-risk site across all low-lying block groups. Among exposed block groups, associations were in general slightly stronger at the 3 km distance between our vulnerability measures and the number of at-risk sites and EAE in 2100.

DISCUSSION

By the end of the century, our analysis projects that 423 potentially hazardous sites in California will be threatened by a 1-in-100 year flood event due to sea level rise if greenhouse gas emissions continue unabated. The majority (88%) of these sites will remain under threat even if greenhouse gas emissions are stabilized and reduced. By 2050, we estimate 129 total sites will be at risk statewide, all but four of which will be at risk under both the low and high emission scenarios because most SLR by midcentury is driven by past rather than future emissions. With their highly industrialized coastlines, the San Francisco Bay Area and Los Angeles/Long Beach regions have the greatest number of at-risk sites.

Oil infrastructure−including actively producing oil and gas wells, refineries, and fossil fuel ports and terminals−makes up a large fraction of the at-risk sites we identified. While flooding after Hurricanes Katrina, Rita, and Harvey was more severe than what might be expected under incremental SLR, these extreme weather events nevertheless provide an indication of the types of contaminant releases that can be expected from flood-damaged oil infrastructure. Flooding following these hurricanes resulted in numerous documented oil spills, pipeline ruptures, and corrosion, as well as excess air pollutant releases during intentional shutdowns, flaring, and start-up operations at petrochemical facilities.[8−11,54,55] Because we did not include pipelines in our analysis, we underestimated the extent of oil and gas infrastructure that may threaten communities with contaminant releases due to SLR. Prior analyses suggest about 90 to 290 km of natural gas pipelines are projected to be flooded by century's end due to SLR in the San Francisco Bay Area alone.[56]

We estimated that nearly a fifth of California's sewage treatment facilities are at-risk by 2100, due to their frequent close proximity to low-lying coastal areas to reduce the cost of discharging treated effluent. A prior study estimated that a 0.9 m (3 feet) SLR flooding scenario in California could affect sewage treatment service to approximately 2.6 million residents.[57] Four counties in the San Francisco Bay Area

https://doi.org/10.1021/acs.est.2c07481
Environ. Sci. Technol. 2023, 57, 7370−7381

(San Francisco, Alameda, Contra Costa, San Mateo, Santa Clara) accounted for the largest proportion of at-risk TRI facilities, in large measure due to the history of industrial development in this region along coastal areas, that includes clusters of diversified economies based on metalworking, oil refining, chemical and pharmaceutical manufacturing, food products, and the semiconductor industry.[58]

In low-lying counties statewide, socially marginalized populations including those with lower levels of voter turnout and higher proportions of residents of color, poor, linguistically isolated households, and households without a vehicle had a higher likelihood of living near an at-risk hazardous facility. These findings are broadly consistent with scholarship on environmental injustice and a report that looked at SLR and contaminated sites listed or being considered for inclusion under the Superfund program along the East and Gulf Coasts. Findings from that analysis concluded that people of color and low-income communities were disproportionately represented among the populations living within 1.6, 4.8, and 8.0 km (1, 3, and 5 miles) of clean up sites at risk of coastal flooding under low, medium, and high SLR scenarios.[59] Another analysis of former hazardous manufacturing facilities in 6 U.S. cities identified more than 6000 "relic" industrial sites with elevated flood risk over the next 30 years (2050), with socially vulnerable groups, including people of color and low income, disproportionately likely to live in these areas.[60] A 2011 study of SLR threats to California infrastructure also found that communities of color were more likely to be affected in areas experiencing potential SLR-related flooding threats,[61] although this analysis examined fewer site and facility categories and assessed fewer scenarios.

Strengths of our study include the use of tax parcel data to better approximate the extent of facility boundaries, a probabilistic approach to estimating SLR-related flood risk, dasymetric mapping to more precisely estimate populations and community demographics near at-risk sites, consideration of SLR-related groundwater rise, and splines to assess non(log)linear associations. Prior studies have shown that utilizing dasymetric mapping methods rather than census-block boundaries results in more accurate estimates of populations at risk of flooding.[62] Prior environmental justice studies have also shown the importance of assessing nonlinear associations in the relationship between demographics and environmental hazards, because they are not always monotonic and assuming a linear relationship may underestimate disparities.[17,63] The involvement of environmental justice collaborators also strengthened the rigor and policy relevance of our analysis. For example, they informed the inclusion criteria for FRS facilities by identifying when important local industrial sites in their community were omitted because of overly strict criteria. The addition of the extreme SLR scenarios and groundwater projections was the result of dialogue with residents in impacted communities and agency officials through a webinar series facilitated by our environmental justice partners. These webinars also served to spark discussion of research and policy priorities to enhance the climate resilience of marginalized populations in California and resulted in the use of our flood risk projections by regulatory agency staff to inform SLR-related planning (personal communication).

Several factors may cause average annual exposure of hazardous sites to diverge from our projections. Our flood models assume that the frequency and magnitude of flood events will remain static over the coming century. However, recent studies suggest that tropical cyclone activity will change, and intensity could increase due to the warming climate,[64−66] leading to even more damaging impacts annually to coastal populations.[67] Additionally, our approach to estimating annual probabilities of flood level exceedance does not consider nonlinear interactions between extreme flood events and local topography (i.e., a "bathtub" approach). In some situations, these dynamics may cause increased flood levels at inland locations, especially where marshlands shrink and land use becomes more developed.[68] Conversely, this approach also does not account for floodwater level attenuation, which may cause us to overestimate exposure during extreme storm events where land is particularly wide and flat.[69,70]

Errors in the secondary data on the location of hazardous sites and industrial facilities may have also caused us to over- or underestimate the number of at-risk sites. We did not consider all types of potentially hazardous sites, omitting for example underground storage tanks, brownfields, and non-National Priority List Superfund sites that may result in contamination releases if flooded. We additionally do not attempt to project future changes in flood risk mitigation or population and demographic shifts, given the uncertainty in trying to predict this information. It is therefore possible that actions to mitigate flood risk near hazardous sites, gentrification, and other factors could change the associations we observed between social vulnerability and proximity to at-risk sites.

Our findings indicate that environmental justice should be prioritized in policy and community-resilience planning related to sea level rise and climate adaptation. Future in-depth site-specific work is needed to more fully characterize the threats posed by flooding at individual locations identified as at-risk in our statewide analysis, including the impact of factors beyond the overland flooding by seawater that was the focus of our analysis. This could include the ways in which increased precipitation due to climate change and groundwater movement due to SLR may contribute to the spread of contaminants and potential exposure threats to nearby communities. Unlike other parts of the country, California's coastline has relatively high elevation, and the state does not typically experience extreme tropical storms or hurricane events. It is therefore likely that SLR-related flooding threats at industrial and hazardous sites are even greater in other regions such as the Gulf and East Coasts and Puerto Rico. Additional research is needed to more systematically identify at-risk sites and nearby vulnerable communities in these regions in order to proactively undertake mitigation measures that prevent contaminant releases due to flooding.

■ ASSOCIATED CONTENT

Supporting Information

The Supporting Information is available free of charge at https://pubs.acs.org/doi/10.1021/acs.est.2c07481.

> Facility inclusion criteria and categorization methods, an illustration of the dasymetric mapping method and study area, facility flood risk and groundwater projections using medium- and high-risk aversion scenarios, correlation coefficients between vulnerability metrics, and full model results for effect estimates shown in Figures 2 and 3 and generalized additive models (PDF)

https://doi.org/10.1021/acs.est.2c07481
Environ. Sci. Technol. 2023, 57, 7370−7381

AUTHOR INFORMATION

Corresponding Authors

Lara J. Cushing − *Department of Environmental Health Sciences, University of California Los Angeles, Los Angeles, California 90095, United States;* orcid.org/0000-0003-0640-6450; Email: lcushing@ucla.edu

Rachel Morello-Frosch − *Department of Environmental Science, Policy and Management & School of Public Health, University of California, Berkeley, Berkeley, California 94720, United States*; Email: rmf@berkeley.edu

Authors

Yang Ju − *School of Architecture and Urban Planning, Nanjing University, Nanjing, China 210093*

Scott Kulp − *Climate Central, Princeton, New Jersey 08542, United States*

Nicholas Depsky − *Energy and Resources Group, University of California, Berkeley, Berkeley, California 94720, United States*

Seigi Karasaki − *Energy and Resources Group, University of California, Berkeley, Berkeley, California 94720, United States*

Jessie Jaeger − *PSE Healthy Energy, Oakland, California 94612, United States*

Amee Raval − *Asian Pacific Environmental Network, Oakland, California 94612, United States*

Benjamin Strauss − *Climate Central, Princeton, New Jersey 08542, United States*

Complete contact information is available at: https://pubs.acs.org/10.1021/acs.est.2c07481

Author Contributions

L.J.C. − Conceptualization, methodology, project administration, funding acquisition, writing−original draft. Y.J. − Data curation, formal analysis, writing−original draft. S.Kulp − Data curation, software, formal analysis, writing−review and editing. N.D. − Data curation, validation, writing−original draft. S.Karasaki − Validation, investigation, data curation, visualization, writing−original draft. J.J. − Data curation, validation. A.R. − Conceptualization, methodology, funding acquisition, writing−review and editing. B.S. − Conceptualization, methodology, funding acquisition, writing−review and editing. R.M.-F. − Conceptualization, methodology, project administration, funding acquisition, writing original draft− review and editing.

Notes

This document has not been formally reviewed by the EPA. The views expressed in this document are solely those of the authors and do not necessarily reflect those of the EPA. The EPA does not endorse any products or commercial services mentioned in this publication.

The authors declare no competing financial interest.

ACKNOWLEDGMENTS

We thank the Toxic Tides Advisory Council−comprised of community leaders from the Asian Pacific Environmental Network, Central Coast Alliance for a Sustainable Economy, Physicians for Social Responsibility Los Angeles, Public Health Institute, and WE ACT for Environmental Justice−for their expertise, guidance, and support throughout this research project. This work was funded by the California Strategic Growth Council (#CCRP0022) awarded to the University of California, Berkeley, the U.S. Environmental Protection Agency (Assistance Agreement No. 84003901 awarded to the University of California Los Angeles), and the JPB and Kresge Foundations. Y.J. is also supported by the "Yuxiu Young Scholars Program" and the Fundamental Research Funds for the Central Universities (#2022300171) at Nanjing University.

REFERENCES

(1) Vitousek, S.; Barnard, P. L.; Fletcher, C. H.; Frazer, N.; Erikson, L.; Storlazzi, C. D. Doubling of Coastal Flooding Frequency within Decades Due to Sea-Level Rise. *Sci. Rep.* **2017**, *7* (1), 1399.

(2) NOAA. *Is sea level rising?*. National Ocean Service website. https://oceanservice.noaa.gov/facts/sealevel.html (accessed 2022-02-11).

(3) Pierce, D. W.; Kalansky, J. F.; Cayan, D. R. *Climate, Drought, and Sea Level Rise Scenarios for California's Fourth Climate Change Assessment*; California Energy Commission: Scripps Institution of Oceanography, La Jolla, CA, 2018; p 78. https://www.energy.ca.gov/sites/default/files/2019-11/Projections_CCCA4-CEC-2018-006_ADA.pdf (accessed 2023-03-24).

(4) Strauss, B.; Tebaldi, C.; Kulp, S.; Cutter, S.; Emrich, C.; Rizza, D.; Yawitz, D. *California, Oregon, Washington and the Surging Sea: A Vulnerability Assessment with Projections for Sea Level Rise and Coastal Flood Risk*; Climate Central Research Report; 2014; pp 1−29. https://riskfinder.climatecentral.org/state/california.us (accessed 2023-03-24).

(5) Cayan, D. R.; Bromirski, P. D.; Hayhoe, K.; Tyree, M.; Dettinger, M. D.; Flick, R. E. Climate Change Projections of Sea Level Extremes along the California Coast. *Clim. Change* **2008**, *87* (S1), 57−73.

(6) Lieberman-Cribbin, W.; Liu, B.; Sheffield, P.; Schwartz, R.; Taioli, E. Socioeconomic Disparities in Incidents at Toxic Sites during Hurricane Harvey. *J. Expo. Sci. Environ. Epidemiol.* **2021**, *31* (3), 454−460.

(7) Stafford, S. L.; Renaud, A. D. Measuring the Potential for Toxic Exposure from Storm Surge and Sea-Level Rise: Analysis of Coastal Virginia. *Nat. Hazards Rev.* **2019**, *20* (1), 04018024-1−04018024-11.

(8) Flores, A. B.; Castor, A.; Grineski, S. E.; Collins, T. W.; Mullen, C. Petrochemical Releases Disproportionately Affected Socially Vulnerable Populations along the Texas Gulf Coast after Hurricane Harvey. *Popul. Environ.* **2021**, *42* (3), 279−301.

(9) Manuel, J. In Katrina's Wake. *Environ. Health Perspect.* **2006**, *114* (1), A32.

(10) Ruckart, P. Z.; Orr, M. F.; Lanier, K.; Koehler, A. Hazardous Substances Releases Associated with Hurricanes Katrina and Rita in Industrial Settings, Louisiana and Texas. *J. Hazard. Mater.* **2008**, *159* (1), 53−57.

(11) Sengul, H.; Santella, N.; Steinberg, L. J.; Cruz, A. M. Analysis of Hazardous Material Releases Due to Natural Hazards in the United States. *Disasters* **2012**, *36* (4), 723−743.

(12) Picou, J. S. Katrina as a Natech Disaster: Toxic Contamination and Long-Term Risks for Residents of New Orleans. *J. Appl. Soc. Sci.* **2009**, *3* (2), 39−55.

(13) Anenberg, S. C.; Kalman, C. Extreme Weather, Chemical Facilities, and Vulnerable Communities in the US Gulf Coast: A Disastrous Combination. *GeoHealth* **2019**, *3* (5), 122−126.

(14) Radke, J.; Biging, G.; Schmidt-Poolman, M.; Foster, H.; Roe, E.; Ju, Y.; Hoes, O.; Beach, T.; Alruheil, A.; Meier, L.; Hsu, W.; Neuhausler, R.; Fourt, W.; Lang, W.; Garcia, U.; Reeves, I. *Assessment of Bay Area Natural Gas Pipeline Vulnerability to Climate Change*; CEC-500-2017-008; California Energy Commission, 2016.

(15) Mohai, P.; Lantz, P. M.; Morenoff, J.; House, J. S.; Mero, R. P. Racial and Socioeconomic Disparities in Residential Proximity to Polluting Industrial Facilities: Evidence From the Americans' Changing Lives Study. *Am. J. Public Health* **2009**, *99* (S3), S649−S656.

(16) Cushing, L.; Faust, J.; August, L. M.; Cendak, R.; Wieland, W.; Alexeeff, G. Racial/Ethnic Disparities in Cumulative Environmental

Health Impacts in California: Evidence From a Statewide Environmental Justice Screening Tool (CalEnviroScreen 1.1). *Am. J. Public Health* **2015**, *105* (11), 2341−2348.
(17) Casey, J. A.; Cushing, L.; Depsky, N.; Morello-Frosch, R. Climate Justice and California's Methane Superemitters: Environmental Equity Assessment of Community Proximity and Exposure Intensity. *Environ. Sci. Technol.* **2021**, *55* (21), 14746−14757.
(18) Morello-Frosch, R.; Lopez, R. The Riskscape and the Color Line: Examining the Role of Segregation in Environmental Health Disparities. *Environ. Res.* **2006**, *102* (2), 181−196.
(19) Pastor, M.; Bullard, R.; Boyce, J. K.; Fothergill, A.; Morello-Frosch, R.; Wright, B. Environment, Disaster, and Race After Katrina. *Race Poverty Environ.* **2006**, *13* (1), 21−26.
(20) Sharkey, P. Survival and Death in New Orleans: An Empirical Look at the Human Impact of Katrina. *J. Black Stud.* **2007**, *37* (4), 482−501.
(21) Bullard, R. D.; Johnson, G. S.; Torres, A. O. Transportation Matters: Stranded on the Side of the Road Before and After Disasters Strike. In *Race, Place, and Environmental Justice after Hurricane Katrina*; Routledge, 2009.
(22) Balazs, C. L.; Morello-Frosch, R. The Three Rs: How Community-Based Participatory Research Strengthens the Rigor, Relevance, and Reach of Science. *Environ. Justice* **2013**, *6* (1), 9−16.
(23) Leydesdorff, L.; Ward, J. Science Shops: A Kaleidoscope of Science−Society Collaborations in Europe. *Public Underst. Sci.* **2005**, *14* (4), 353−372.
(24) O'Fallon, L. R.; Dearry, A. Community-Based Participatory Research as a Tool to Advance Environmental Health Sciences. *Environ. Health Perspect.* **2002**, *110* (suppl 2), 155−159.
(25) US EPA. *Facility Registry Service (FRS)*. US EPA. https://www.epa.gov/frs (accessed 2019-03-07).
(26) *Layer Information for Interactive State Maps*. U.S. Energy Information Administration. https://www.eia.gov/maps/layer_info-m.php (accessed 2020-11-17).
(27) *WCSC Waterborne Commerce Statistics Center*. US Army Corps of Engineers Institute for Water Resources Website. https://www.iwr.usace.army.mil/About/Technical-Centers/WCSC-Waterborne-Commerce-Statistics-Center-2/ (accessed 2020-12-23).
(28) Enverus | *Creating the future of energy together*. https://www.enverus.com/ (accessed 2023-03-24).
(29) Nationwide Parcel Data & Property Level Geocodes | *SmartParcels®*. Digital Map Products Lightbox. https://www.digmap.com/platform/smartparcels/ (accessed 2020-07-01).
(30) Kulp, S.; Strauss, B. H. Rapid Escalation of Coastal Flood Exposure in US Municipalities from Sea Level Rise. *Clim. Change* **2017**, *142* (3), 477−489.
(31) Buchanan, M. K.; Kulp, S.; Cushing, L.; Morello-Frosch, R.; Nedwick, T.; Strauss, B. Sea Level Rise and Coastal Flooding Threaten Affordable Housing. *Environ. Res. Lett.* **2020**, *15* (12), 124020.
(32) Kopp Robert, E.; Horton Radley, M.; Little Christopher, M.; Mitrovica Jerry, X.; Oppenheimer, M.; Rasmussen, D. J.; Strauss Benjamin, H.; Tebaldi, C. Probabilistic 21st and 22nd Century Sea-level Projections at a Global Network of Tide-gauge Sites. *Earths Future* **2014**, *2* (8), 383−406.
(33) Tebaldi, C.; Strauss, B. H.; Zervas, C. E. Modelling Sea Level Rise Impacts on Storm Surges along US Coasts. *Environ. Res. Lett.* **2012**, *7* (1), 014032.
(34) NOAA. *Digital Coast Data*. Office for Coastal Management Digital Coast. https://coast.noaa.gov/digitalcoast/data/home.html (accessed 2022-07-20).
(35) Ocean Protection Council. *State of California Sea-Level Rise Guidance - 2018 Update*; p 84. https://opc.ca.gov/webmaster/ftp/pdf/agenda_items/20180314/Item3_Exhibit-A_OPC_SLR_Guidance-rd3.pdf (accessed 2023-03-24).
(36) California Coastal Commission *California Coastal Commission Sea Level Rise Policy Guidance*; 2018; p 307.
(37) Loáiciga, H. A.; Pingel, T. J.; Garcia, E. S. Sea Water Intrusion by Sea-Level Rise: Scenarios for the 21st Century. *Groundwater* **2012**, *50* (1), 37−47.
(38) Plane, E.; Hill, K.; May, C. A Rapid Assessment Method to Identify Potential Groundwater Flooding Hotspots as Sea Levels Rise in Coastal Cities. *Water* **2019**, *11* (11), 2228.
(39) Befus, K. M.; Hoover, D. J.; Erikson, L. H. *Projected Groundwater Emergence and Shoaling for Coastal California Using Present-Day and Future Sea-Level Rise Scenarios*; DOI: 10.5066/P9H5PBXP.
(40) Our Coast, Our Future. *Science and Modeling*. https://ourcoastourfuture.org/science-and-modeling/ (accessed 2022-04-19).
(41) US Census Bureau. *2013−2017 ACS 5-year Estimates*. https://www.census.gov/programs-surveys/acs/technical-documentation/table-and-geography-changes/2017/5-year.html (accessed 2023-03-24).
(42) Nordby, H.; Vaisman, E.; Williams, S. *Naturally Occurring Affordable Housing*; Technical Report 2; CoStar and Urban Land Institute, 2017; pp 1−10.
(43) *Statewide Database | Election Data*. https://statewidedatabase.org/election.html (accessed 2020-07-01).
(44) Maizlish, N. *Technical Documentation: California Health Disadvantage Index (HDI 1.1)*; Public Health Alliance of Southern California, 2016; p 38.
(45) August, L. *CalEnviroScreen 4.0*; OEHHA. https://oehha.ca.gov/calenviroscreen/report/calenviroscreen-40 (accessed 2023-03-24).
(46) OEHHA. *SB 535 Disadvantaged Communities*; California Office of Environmental Health Hazard Assessment. https://oehha.ca.gov/calenviroscreen/sb535 (accessed 2023-03-24).
(47) Clough, E.; Bell, D. Just Fracking: A Distributive Environmental Justice Analysis of Unconventional Gas Development in Pennsylvania, USA. *Environ. Res. Lett.* **2016**, *11* (2), 025001.
(48) Mitsova, D.; Esnard, A.-M.; Li, Y. Using Enhanced Dasymetric Mapping Techniques to Improve the Spatial Accuracy of Sea Level Rise Vulnerability Assessments. *J. Coast. Conserv.* **2012**, *16* (3), 355−372.
(49) Pace, C.; Balazs, C.; Cushing, L. J.; Goddard, J. J.; Morello-Frosch, R. An Equity Analysis of Drinking Water Quality and Source Vulnerability in California. *Am. J. Public Health* 2022.
(50) Depsky, N. J.; Cushing, L.; Morello-Frosch, R. High-Resolution Gridded Estimates of Population Sociodemographics from the 2020 Census in California. *PLoS One* **2022**, *17* (7), e0270746.
(51) Microsoft/USBuildingFootprints, 2019. https://github.com/microsoft/USBuildingFootprints (accessed 2019-09-16).
(52) Molitor, J.; Su, J. G.; Molitor, N.-T.; Rubio, V. G.; Richardson, S.; Hastie, D.; Morello-Frosch, R.; Jerrett, M. Identifying Vulnerable Populations through an Examination of the Association Between Multipollutant Profiles and Poverty. *Environ. Sci. Technol.* **2011**, *45* (18), 7754−7760.
(53) Sadd, J. L.; Pastor, M.; Morello-Frosch, R.; Scoggins, J.; Jesdale, B. Playing It Safe: Assessing Cumulative Impact and Social Vulnerability through an Environmental Justice Screening Method in the South Coast Air Basin, California. *Int. J. Environ. Res. Public. Health* **2011**, *8* (12), 1441−1459.
(54) Santella, N.; Steinberg, L. J.; Sengul, H. Petroleum and Hazardous Material Releases from Industrial Facilities Associated with Hurricane Katrina. *Risk Anal.* **2010**, *30* (4), 635−649.
(55) Davis, A.; Thrift-Viveros, D.; Baker, C. M. S. NOAA Scientific Support for a Natural Gas Pipeline Release During Hurricane Harvey Flooding in the Neches River Beaumont, Texas. *Int. Oil Spill Conf. Proc.* **2021**, *2021* (1), 687018.
(56) Ju, Y.; Lindbergh, S.; He, Y.; Radke, J. D. Climate-Related Uncertainties in Urban Exposure to Sea Level Rise and Storm Surge Flooding: A Multi-Temporal and Multi-Scenario Analysis. *Cities* **2019**, *92*, 230−246.
(57) Hummel, M. A.; Berry, M. S.; Stacey, M. T. Sea Level Rise Impacts on Wastewater Treatment Systems Along the U.S. Coasts. *Earths Future* **2018**, *6* (4), 622−633.

https://doi.org/10.1021/acs.est.2c07481
Environ. Sci. Technol. 2023, 57, 7370−7381

(58) Walker, R.; Schafran, A. The Strange Case of the Bay Area. *Environ. Plan. Econ. Space* **2015**, *47* (1), 10−29.
(59) Carter, J.; Kalman, C. A Toxic Relationship, 2020. https://www.ucsusa.org/resources/toxic-relationship (accessed 2023-03-24).
(60) Marlow, T.; Elliott, J. R.; Frickel, S. Future Flooding Increases Unequal Exposure Risks to Relic Industrial Pollution. *Environ. Res. Lett.* **2022**, *17* (7), 074021.
(61) Heberger, M.; Cooley, H.; Herrera, P.; Gleick, P. H.; Moore, E. Potential Impacts of Increased Coastal Flooding in California Due to Sea-Level Rise. *Clim. Change* **2011**, *109* (1), 229−249.
(62) Maantay, J.; Maroko, A. Mapping Urban Risk: Flood Hazards, Race, & Environmental Justice in New York. *Appl. Geogr.* **2009**, *29*, 111−124.
(63) Daouda, M.; Henneman, L.; Goldsmith, J.; Kioumourtzoglou, M.-A.; Casey, J. A. Racial/Ethnic Disparities in Nationwide PM2.5 Concentrations: Perils of Assuming a Linear Relationship. *Environ. Health Perspect.* **2022**, *130* (7), 077701.
(64) Knutson, T. R.; Sirutis, J. J.; Vecchi, G. A.; Garner, S.; Zhao, M.; Kim, H.-S.; Bender, M.; Tuleya, R. E.; Held, I. M.; Villarini, G. Dynamical Downscaling Projections of Twenty-First-Century Atlantic Hurricane Activity: CMIP3 and CMIP5Model-Based Scenarios. *J. Clim.* **2013**, *26* (17), 6591−6617.
(65) Emanuel, K. A. Downscaling CMIP5 Climate Models Shows Increased Tropical Cyclone Activity over the 21st Century. *Proc. Natl. Acad. Sci. U. S. A.* **2013**, *110* (30), 12219−12224.
(66) Emanuel, K. Response of Global Tropical Cyclone Activity to Increasing CO2: Results from Downscaling CMIP6Models. *J. Clim.* **2021**, *34* (1), 57−70.
(67) Geiger, T.; Gütschow, J.; Bresch, D. N.; Emanuel, K.; Frieler, K. Double Benefit of Limiting Global Warming for Tropical Cyclone Exposure. *Nat. Clim. Change* **2021**, *11* (10), 861−866.
(68) Bilskie, M. V.; Hagen, S. C.; Alizad, K. A.; Medeiros, S. C.; Passeri, D.; Needham, H. F.; Cox, A. Dynamic Simulation and Numerical Analysis of Hurricane Storm Surge under Sea Level Rise with Geomorphologic Changes along the Northern Gulf of Mexico. *Earth's Future* **2016**, *4*, 177−193.
(69) Gallien, T. W.; Sanders, B. F.; Flick, R. E. Urban Coastal Flood Prediction: Integrating Wave Overtopping, Flood Defenses and Drainage. *Coast. Eng.* **2014**, *91*, 18−28.
(70) Vafeidis, A. T.; Schuerch, M.; Wolff, C.; Spencer, T.; Merkens, J. L.; Hinkel, J.; Lincke, D.; Brown, S.; Nicholls, R. J. Water-Level Attenuation in Global-Scale Assessments of Exposure to Coastal Flooding: A Sensitivity Analysis. *Nat. Hazards Earth Syst. Sci.* **2019**, *19* (5), 973−984.

https://doi.org/10.1021/acs.est.2c07481
Environ. Sci. Technol. 2023, 57, 7370−7381